CHINESE OPTICS LETTERS

Vol. 22, No. 1 | January 2024

Pulse repetition rate effect on the plasma inside femtosecond laser filament in air

Fukang Yin (尹富康)[1,2], Tie-Jun Wang (王铁军)[1,2*], Yaoxiang Liu (刘尧香)[1], Juan Long (龙 娟)[1,2], Yingxia Wei (魏迎霞)[1], Bin Zhu (朱 斌)[3], Kainan Zhou (周凯南)[3], and Yuxin Leng (冷雨欣)[1,2]

[1] State Key Laboratory of High Field Laser Physics, Shanghai Institute of Optics and Fine Mechanics and CAS Center for Excellence in Ultra-intense Laser Science, Chinese Academy of Sciences, Shanghai 201800, China

[2] Center of Materials Science and Optoelectronics Engineering, University of Chinese Academy of Sciences, Beijing 100049, China

[3] Laser Fusion Research Center and Science & Technology on Plasma Physics Laboratory, China Academy of Engineering Physics, Mianyang 621999, China

*Corresponding author: tiejunwang@siom.ac.cn

Received July 21, 2023 | Accepted August 18, 2023 | Posted Online January 8, 2024

The characteristics of plasmas play an important role in femtosecond laser filament-based applications. Spectroscopic analysis is used to experimentally investigate the plasma density and its temperature of the air filament under different pulse repetition rates. In our experiments, the measured average plasma density of the filament is 1.54×10^{17} cm^{-3} and the temperature of the plasma is about 5100 K under 100 Hz pulse repetition rate. The plasma density decreases to 1.43×10^{17} cm^{-3} and the temperature increases to 6230 K as the pulse repetition rate increases to 1000 Hz. The experimental observation agrees with the numerical simulation by solving the nonlinear Schrödinger equations with repetition rate related "low density hole" correction.

Keywords: femtosecond laser filamentation; cumulative effects; electron density.
DOI: 10.3788/COL202422.013201

1. Introduction

The propagation of powerful femtosecond laser pulses in air is a very complicated phenomenon that involves a number of nonlinear processes, including four- and six-wave mixing[1,2], odd harmonics[3,4], self-focusing and filamentation[5], self-phase modulation[6], supercontinuum generation[7,8], and so on. The self-focusing phenomenon during the nonlinear propagation leads to the ionization of air molecules. The dynamic balance between self-focusing, owing to the Kerr effect, and plasma defocusing results in the formation of laser plasma filament, which stabilizes laser pulse parameters (beam diameter and pulse duration) in the filament[9]. Due to its unique properties, femtosecond laser filamentation finds applications in remote spectroscopy[10] and fabrication[11], air lasing[12], fuel ignition[13], and combustion diagnostics[14]. Furthermore, the plasmas ionized by the laser pulse have a significant impact on all of the nonlinear processes mentioned above as well as for the related applications in practice[10,15]. Therefore, from both scientific and practical perspectives, it is crucial to have the femtosecond laser pulses produce the plasma properties in the filaments. So far, the plasma density and electron temperature inside the filaments in air have been measured and analyzed mostly in the case of air excitation by the femtosecond laser pulses under a single repetition rate[16–18]. Recently, laser repetition-related THz production[11], wake dynamics[19], fluorescence[20], clamping intensity[21], and the cumulative effects[22] from air filaments have been reported as high-energy, ultrashort, high-repetition-rate laser systems become commercially accessible. Through pump-probe experiments[23], we recently found that the low-density region, due to the accumulative effect by 1 kHz repetition filaments, results in higher plasma density obtained in the measurements. However, the pulse repetition effect on the laser ionized plasmas inside femtosecond air filaments is not fully explored yet.

In this Letter, the pulse repetition rate effect on the plasma temperature and density was studied using spectroscopic analysis of the side fluorescence from a femtosecond laser plasma filament in air. Laser exciting oxygen atomic fluorescence lines at 777 nm and 844 nm were employed to look into the plasma density and temperature using the Stark broadening effect and Boltzmann plot[18]. The plasma density decreases, and the plasma temperature increases as the laser repetition rate increases from 100 Hz to 1 kHz. Numerical simulation based on nonlinear Schrödinger equations was performed to support the experimental observations.

2. Experimental Setup

Figure 1 shows an experimental setup designed particularly to monitor the side fluorescence produced by oxygen from a laser-created air plasma filament. In the experiments, the ultrafast laser pulses (duration 35 fs, pulse energy 4.5 mJ, repetition rate up to 1 kHz) produced by a Ti:sapphire laser amplifier were focused in the air by an $f = 30$ cm plano-convex lens (L_1) to generate laser filaments (Fig. 1). The radius of the laser beam waist was about 7 mm (1/e). The oxygen atomic fluorescence in the near-infrared band emitted by the filament was imaged from the side into the slit of a spectrometer. The imaging system consisted of a pair of lenses, L_2 and L_3 (30 cm and 10 cm focal lengths, respectively), and a pair of orthogonally placed aluminum mirrors. The height of the fluorescence propagation plane of the filament was lowered and the filament fluorescence was rotated vertically to be parallel to the slit of the spectrometer by the pair of aluminum mirrors. To remove the secondary spectrum of the spectrometer, a long pass filter cut at 550 nm was placed in front of the spectrometer slit. An intensified charge-coupled device (ICCD) mounted on the spectrometer trigged by the laser system was used to capture the fluorescence spectrum generated by the filament. The gate width of the ICCD was set as 10 ns. The delay of the ICCD gate with respect to the laser arrival was 0, which ensures all the fluorescence was collected. 15,000 laser shots were accumulated and averaged for the spectral analysis. A 1200 grooves/mm grating of the spectrometer was chosen for measuring the Stark broadening data of the O I (777.4 nm and 844.3 nm) lines. To precisely monitor the laser energy at different repetition rates, an energy meter (Ophir PE50-DIF-C) was inserted after the lens L_1.

3. Results and Discussion

The typical spectra in the near-infrared band emitted by the filament are shown in Fig. 2. The principles of laser induced breakdown spectroscopy were used to analyze the side-emitted fluorescence line width of the filament. The instrumental broadening was equivalent to 50 pm determined by the full-width at half-maximum (FWHM) of the spectral lines Ar I 750.387 nm and Ar I 772.376 nm produced from a mercury argon lamp. Compared with the measured line width, natural broadening was assumed to be negligible. A multi-Voigt fit considering Stark broadening by Lorentzian profiles and instrumental broadening (0.05 nm, fixed) by Gaussian profiles was performed, as shown in Fig. 2. The spectral bandwidth of the O I (777.19 nm) line was utilized to determine the electron density. The plasma density was estimated by using the FWHM of the spectral line according to the empirical formula[24],

$$N_e = \frac{\Delta\lambda}{2\omega} \times 10^{16}\ \mathrm{cm}^{-3}, \tag{1}$$

where N_e is the density of plasma, $\Delta\lambda$ is the Stark broadening obtained from the O I (777.19 nm) line, and $\omega = 0.0166$ nm is the electron broadening parameter for the O I (777.19 nm) line[16]. The measured plasma densities of the filaments generated by different repetition rates laser pulses are shown in Fig. 3(b). The measured average plasma density of the 100 Hz filament is $1.54 \times 10^{17}\ \mathrm{cm}^{-3}$. The plasma density of the filament decreases with the increase of the filament repetition rate. The measured average plasma density of the 1000 Hz filament decreases by ~10%, down to $1.43 \times 10^{17}\ \mathrm{cm}^{-3}$. The measured plasma density is in agreement with Refs. [17,18] under similar conditions.

Numerical simulations on the laser filamentation in air under different laser repetition rates were performed by solving the nonlinear Schrödinger equations corrected by the "low density hole"[21]. The equations read as

$$\frac{\partial E}{\partial z} = i\frac{1}{2k_0}\Delta_\perp E - i\frac{k''}{2}\frac{\partial^2 E}{\partial t^2} + i\frac{\omega_0}{c}n_2 E - \frac{\beta^K}{2}I^{K-1}E - \frac{\sigma}{2}(1 + i\omega_0\tau)\rho E + ik_0\Delta n E, \tag{2}$$

$$\frac{\partial \rho}{\partial t} = \frac{\beta^K}{K\hbar\omega_0}\left(1 - \frac{\rho}{\rho_{\mathrm{air}}}\right)I^K. \tag{3}$$

The values of the parameters in Eqs. (2) and (3) vary with the air density,

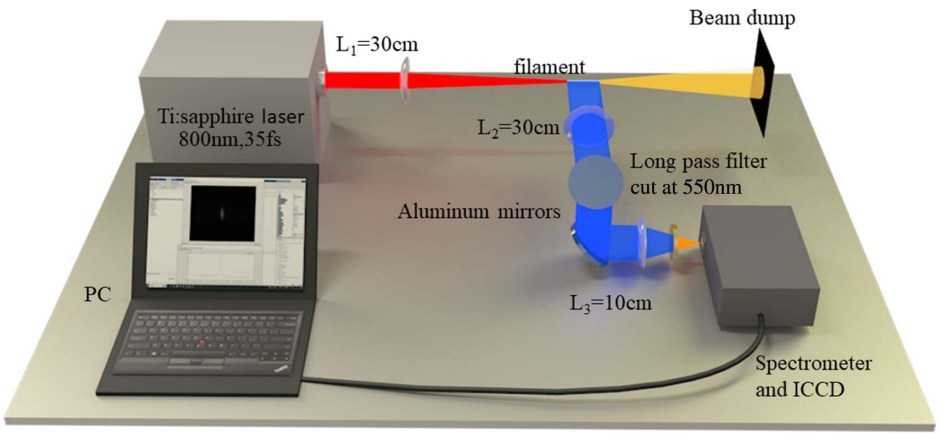

Fig. 1. Experimental setup for characterizing the plasma in the filament under different repetition rates using spectroscopy.

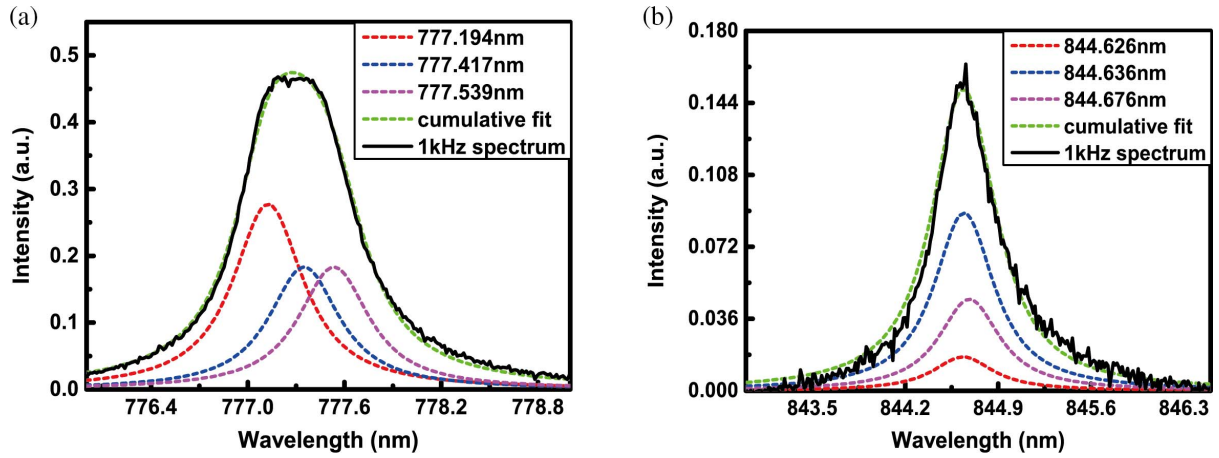

Fig. 2. Typical spectra of the O I line generated by the laser filament. (a) Multi-Voigt fit for the O I 777.194 nm, 777.417 nm, and 777.539 nm lines was performed to determine the Stark broadening of the plasma. (b) Multi-Voigt fit for the O I 844.626 nm, 844.636 nm, and 844.676 nm lines. The six O I spectral lines were used to plot Boltzmann plot and determine the temperature of the plasma. The laser pulse energy was 4.5 mJ for filamentation.

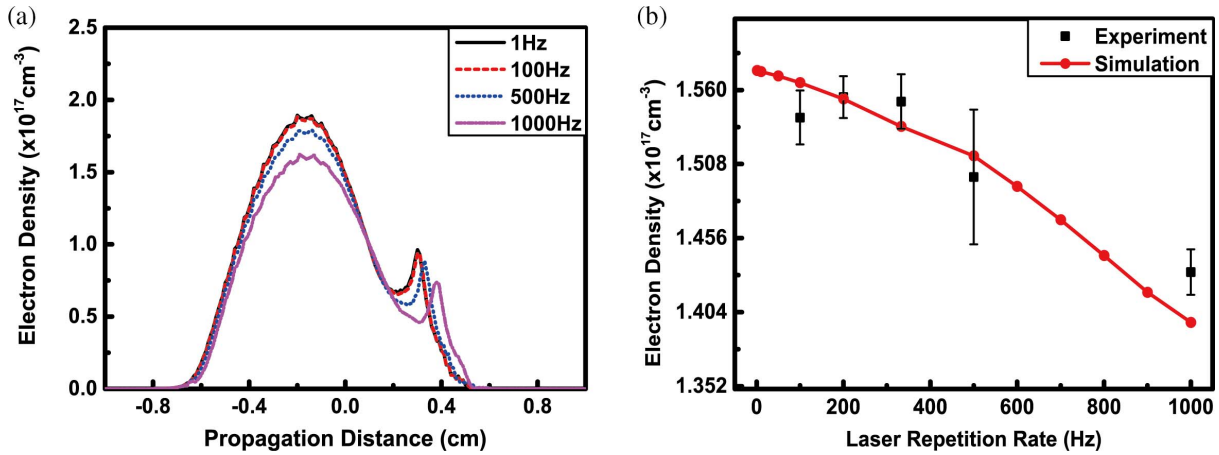

Fig. 3. (a) Simulated average electron density of the filament as a function of the propagation distance for 1 Hz, 100 Hz, 500 Hz, and 1000 Hz repetition rates. The electron density is averaged in the range of $r < 50$ μm (the radius of the filament). (b) Electron density of the laser filament as a function of the laser repetition rate. The red line is the simulated average electron density of the filament zone. The filament zone is defined by specifying the filamentation initiation and termination when the electron density approaches 1×10^{17} cm^{-3}.

$$\tau = \tau_0/\rho_{\text{index}}, \quad \sigma = \sigma_0 \times \frac{\rho_{\text{index}}(1+\omega_0^2\tau_0^2)}{\rho_{\text{index}}^2+\omega_0^2\tau_0^2},$$
$$\beta^K = \beta_0^K \times \rho_{\text{index}}, \quad n_2 = n_{2,0} \times \rho_{\text{index}},$$
$$k'' = k_0'' \times \rho_{\text{index}}, \tag{4}$$

where $\rho_{\text{index}} = \rho_{\text{air}}/\rho_{\text{at}}$ denotes the relative air density[21]. When the ambient air is under 1 atm, the nonlinear coefficient of the Kerr effect is $n_{2,0} = 3.2 \times 10^{-23}$ m^2/W, the momentum transfer collision time is $\tau_0 = 350$ fs, the cross section for the inverse bremsstrahlung is $\sigma_0 = 2 \times 10^{-24}$ m^2, the coefficient related to the multiphoton ionization is $\beta_0^K = 1.27 \times 10^{-160}$ m^{17}/W^9, and the coefficient of group velocity dispersion is $k_0''= 2 \times 10^{-29}$ s^2/m.

The process of heating caused by filamentation can be regarded as an isochoric (constant volume) process[25]. The peak temperature variation ΔT_{peak} through plasma recombination in air is calculated as[21]

$$\Delta T_{\text{peak}}(z) = \frac{U\rho_{\text{plasma}}(r=0,z)}{c_v\rho_{\text{at}}}, \tag{5}$$

where the ionization potential energy for the air molecules is $U = 14.6$ eV. $\rho_{\text{plasma}}(z)$ is the longitudinal distribution of the plasma density in the single-pulse case, and c_v is the gas isochoric heat capacity per molecule. The ambient air under 1 atm can be approximately regarded as an ideal diatomic molecular gas, and $c_v = 5k_B/2$. $k_B = 1.38 \times 10^{-23}$ J/K is the Boltzmann constant. ρ_{at} is the neutral molecule density in the air under 1 atm.

The air density of the density hole induced by the energy deposition in the air is described as[21]

$$\rho_{\mathrm{air}}(z) = \rho_{\mathrm{at}} - \Delta\rho_{\mathrm{air}}^{\mathrm{peak}}(z)\exp\left(-\frac{r^2}{R(z)^2}\right), \tag{6}$$

$$\Delta\rho_{\mathrm{air}}^{\mathrm{peak}}(z) = \rho_{\mathrm{at}}\frac{\Delta T_{\mathrm{peak}}(z)R_0^2(z)}{(\Delta T_{\mathrm{peak}}(z) + T_a)R^2(z)}, \tag{7}$$

where $T_a = 300\,\mathrm{K}$ is the ambient air temperature, and $R(z) = (R_0^2(z) + 4\alpha\Delta t)^{1/2}$ is the radius of the density hole. The initial radius of the density hole $R_0(z)$ is the radial distribution of air density in FWHM at the z position. Then, the "low density hole" will evolve with the thermal diffusivity $\alpha = 0.19\,\mathrm{cm}^2/\mathrm{s}$[26,27]. Δt is the pulse temporal spacing of the subsequent pulse.

The refractive index change contributed by the density hole is written as[27]

$$\Delta n(z) = -\Delta n_m(z)\exp\left(-\frac{r^2}{R^2(z)}\right), \tag{8}$$

$$\Delta n_m(z) = (n_0 - 1)\frac{\Delta T_{\mathrm{peak}}(z)}{T_a}\frac{R_0^2(z)}{R^2(z)}, \tag{9}$$

where $n_0 = 1.000275$ is the refractive index of the ambient air, and Δn_m is the maximal refractive index change[27].

The initial laser beam is assumed to be Gaussian type as described by

$$E = E_0\exp(-r^2/w_0^2)\exp(-t^2/\tau_p^2)\exp(-ik_0r^2/2f). \tag{10}$$

In our experiment, the waist of the initial beam is $w_0 = 7\,\mathrm{mm}$, the pulse duration is $\tau_p = 35\,\mathrm{fs}$, and the focal length is $f = 30\,\mathrm{cm}$.

Both experimental and theoretical results [Fig. 3(b)] show that the average plasma density of the filament zone decreases with the increase of the laser repetition rate, which confirms that the repetition-rate dependent low-density hole plays a significant role in the ionization of air molecules during the process of laser filamentation in air. The low-density hole will cause a smaller nonlinear refractive index coefficient and lower ionization rate. The effect caused by the low-density hole is enhanced with the increase of the laser repetition rate, which is due to the shorter pulse interval time.

The two key parameters in comprehending the intricate phenomena occurring in plasma are electron temperature and its density. When the plasma is in the local thermal equilibrium (LTE) condition, these parameters can be measured. The LTE condition of plasma was justified by the fulfillment of the McWhirter criterion, which describes the minimum plasma density required for the plasma to be in the LTE state. The McWhirter criterion reads[28]

$$N_e \geq N_{\mathrm{cr}} = 1.6\times10^{12}\sqrt{T}(\Delta E)^3, \tag{11}$$

where T (in K) is the temperature of the plasma, ΔE (in eV) is the largest gap between adjacent energy levels, and N_{cr} is the critical density for the LTE. In the case of the O I (777.4 nm) line, the energy gap is about 1.59 eV, and the temperature of the plasma in the filament is about 5000 K. The minimum plasma density required to satisfy the McWhirter criterion is about $4.5\times10^{14}\ \mathrm{cm}^{-3}$. The average plasma density of the filament zone is above $1.4\times10^{17}\ \mathrm{cm}^{-3}$, which satisfies the McWhirter criterion [Eq. (11)].

In the LTE condition, the plasma temperature is the electron temperature[29], not the thermal temperature. The plasma temperature can be determined by applying the formula to the intensity of the spectral lines for a transition from an upper level k to lower level i[30],

$$\ln\left(\frac{I_{ki}\lambda_{ki}}{g_kA_{ki}}\right) = -\frac{E_k}{k_BT} + C, \tag{12}$$

where λ_{ki} is the emission wavelength, I_{ki} is the integral intensity of the emission line, g_k is the degeneracy of the upper-level energy, A_{ki} is the transition probability, E_k is the energy of the upper-level k, $k_B = 1.38\times10^{-23}\,\mathrm{J/K}$ is the Boltzmann constant, and C is a constant. In order to determine the temperature, neutral atomic O I lines were used. The spectroscopic information for A_{ki}, E_k, and g_k of the O I spectral lines is indexed from the National Institute of Standards and Technology (NIST) database[31]. The Boltzmann plot was drawn according to Eq. (12) based on the O I triplet centered at 777.4 nm and 844.6 nm, as shown in Fig. 4(a). The plasma temperature was obtained by fitting the line in the Boltzmann plot, as shown in Fig. 4. The plasma temperature is obtained through the slope $(-\frac{1}{k_BT})$. The slope $(-\frac{1}{k_BT})$ from the 100 Hz filament is more inclined than that of the 1 kHz filament in the Boltzmann plot, which indicates that the plasma temperature of the 1 kHz filament is higher than that of the 100 Hz. The measured plasma temperature of the 100 Hz filament is ~5100 K. The plasma temperature increases with the increase of the laser repetition rate, as shown in Fig. 4(b). The measured plasma temperature of the 1000 Hz filament increases by 22% up to ~6230 K, which is beneficial for plasma filament-related applications, such as air lasing[12], three harmonic generation[23], and supercontinuum generation[8]. The measured plasma temperature is in agreement with Ref. [18] under the similar conditions. The numerically obtained average intensities of the filament zone under different laser repetition rates are shown in Fig. 4(b). The variation trend of the average intensities of different repetition rate filaments agrees with that of the plasma temperature. After the ionization of air molecules, free electrons are accelerated in the laser field. The free electrons gain more energy under a high-repetition rate due to the higher intensity inside the filament[21], which results in a higher plasma temperature.

The effect of the pulse repetition rate on the plasma inside the filament can be understood as the following. The laser energy is deposited into air molecules through the ionization and the fast recombination of the plasmas (~10 ns) inside the filament zone. A high temperature and pressure zone is formed after ionization. Subsequently, the shock wave is formed (~1 μs). The pressure recovers to the environment level at millisecond time scales.

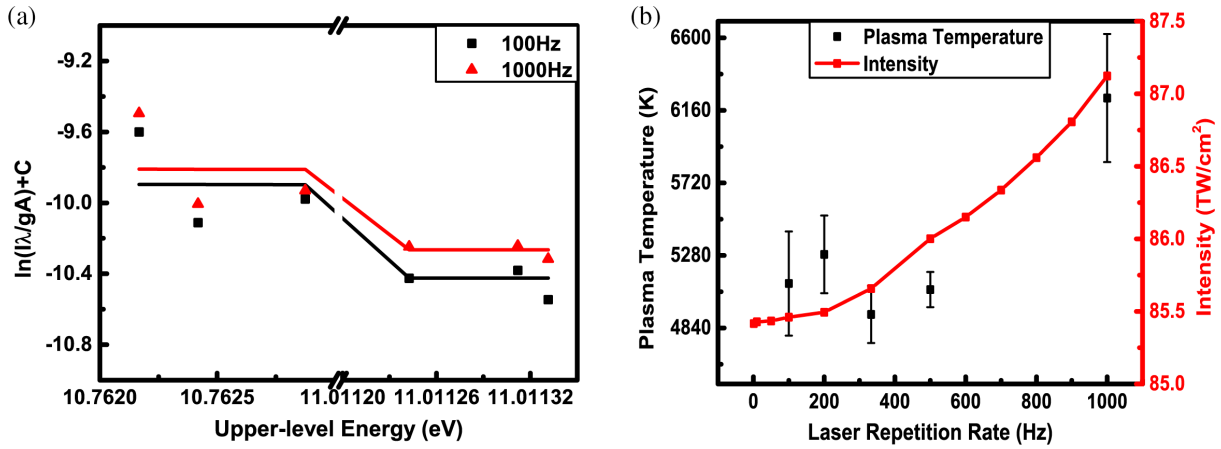

Fig. 4. (a) Boltzmann plots for O I lines from 100 Hz and 1000 Hz filaments. (b) Plasma temperature as a function of the laser repetition rate. The red line in (b) is the simulated laser intensity inside the filament for comparison. The laser pulse energy was 4.5 mJ for filamentation.

According to the ideal gas equation, the gas density distribution is opposite the temperature distribution. A low-density zone is formed and weakened over time. For a higher repetition-rate laser with a pulse interval time that is shorter than the thermal diffusion time, the succeeding pulse propagating in the zone experiences the lower air density zone as well as the lower ionization rate. As a result, fewer air molecules are ionized, as shown in Fig. 3, and less laser energy is spent on the ionization in the filament. The intensity inside the filament is higher. The free electrons from the ionization of the air molecules gain more energy under the high repetition rate due to the higher intensity. The plasma temperature is increased under the high pulse repetition rate, as observed in Fig. 4.

Note that when keeping the laser pulse energy constant and increasing the laser repetition rate, the laser power will increase. As a consequence, a decrease in plasma density and an increase in plasma temperature were observed in this work. When keeping the laser repetition rate constant and increasing the laser pulse energy, the laser power will increase too. Then, an increase in both plasma density and plasma temperature was observed in the literature[19].

4. Conclusion

In summary, we have carried out a spectroscopic analysis of the side fluorescence produced by oxygen from a laser-ionized air plasma filament under different pulse repetition rates. The plasma temperature and its density were estimated through the atomic fluorescence produced by the oxygen. The measured plasma density decreases by 10% from 1.54×10^{17} cm^{-3} to 1.43×10^{17} cm^{-3}, and the temperature of the plasma increases by 22% from 5100 K to 6230 K when the filament pulse repetition rate increases from 100 Hz to 1000 Hz. Nonlinear Schrödinger equations based on numerical simulation results indicate the low-density hole, resulting from the pulse cumulative effect of the high repetition rate filament, which leads to a lower ionization rate. Under a higher pulse repetition rate, the effect caused by the low-density hole is enhanced due to the shorter pulse interval time. Consequently, the plasma density of the laser filament is lower, and the intensity inside the filament is higher for the higher repetition rate filament. The temperature of the plasma is higher due to the free electrons that are accelerated in a higher laser field. We believe that the results not only improve the understanding of the laser repetition effect on the laser filamentation in air but also provide scientific guidance for high repetition rate filament applications.

Acknowledgements

The work was in part supported by the NSAF (No. U2130123), the International Partnership Program of Chinese Academy of Sciences (Nos. 181231KYSB20200033 and 181231KYSB20200040), and the Shanghai Science and Technology Program (No. 21511105000).

References

1. F. Théberge, N. Aközbek, W. Liu, *et al.*, "Tunable ultrashort laser pulses generated through filamentation in gases," Phys. Rev. Lett. **97**, 023904 (2006).
2. V. Vaičaitis, V. Jarutis, K. Steponkevičius, *et al.*, "Noncollinear six-wave mixing of femtosecond laser pulses in air," Phys. Rev. A **87**, 063825 (2013).
3. H. Yang, J. Zhang, J. Zhang, *et al.*, "Third-order harmonic generation by self-guided femtosecond pulses in air," Phys. Rev. E **67**, 015401(R) (2003).
4. A. V. Mitrofanov, A. A. Voronin, S. I. Mitryukovskiy, *et al.*, "Mid-infrared-to-mid-ultraviolet supercontinuum enhanced by third-to-fifteenth odd harmonics," Opt. Lett. **40**, 2068 (2015).
5. A. Braun, G. Korn, X. Liu, *et al.*, "Self-channeling of high-peak-power femtosecond laser pulses in air," Opt. Lett. **20**, 73 (1995).
6. L. Bergé, S. Skupin, R. Nuter, *et al.*, "Ultrashort filaments of light in weakly ionized, optically transparent media," Rep. Prog. Phys. **70**, 1633 (2007).
7. A. K. Dharmadhikari, S. Edward, J. A. Dharmadhikari, *et al.*, "On the generation of polarization-dependent supercontinuum and third harmonic in air," J. Phys. B: At. Mol. Opt. Phys. **48**, 094012 (2015).
8. N. Chen, T.-J. Wang, Z. Zhu, *et al.*, "Laser ellipticity-dependent supercontinuum generation by femtosecond laser filamentation in air," Opt. Lett. **45**, 4444 (2020).

9. A. Becker, N. Aközbek, K. Vijayalakshmi, *et al.*, "Intensity clamping and refocusing of intense femtosecond laser pulses in nitrogen molecular gas," Appl. Phys. B **73**, 287 (2001).
10. H. Xu, Y. Cheng, S.-L. Chin, *et al.*, "Femtosecond laser ionization and fragmentation of molecules for environmental sensing," Laser Photon. Rev. **9**, 275 (2015).
11. Y. Su, S. Wang, D. Yao, *et al.*, "Stand-off fabrication of irregularly shaped, multi-functional hydrophobic and antireflective metal surfaces using femtosecond laser filaments in air," Appl. Surface Sci. **494**, 1007 (2019).
12. P. Polynkin and Y. Cheng, *Air Lasing*, Springer Series in Optical Sciences, Vol. **208** (Springer International Publishing, 2018).
13. H. Zang, H. Li, W. Zhang, *et al.*, "Robust and ultralow-energy-threshold ignition of a lean mixture by an ultrashort-pulsed laser in the filamentation regime," Light Sci. Appl. **10**, 49 (2021).
14. H.-L. Li, H.-L. Xu, B.-S. Yang, *et al.*, "Sensing combustion intermediates by femtosecond filament excitation," Opt. Lett. **38**, 1250 (2013).
15. J. Kasparian, M. Rodriguez, G. Méjean, *et al.*, "White-light filaments for atmospheric analysis," Science **301**, 61 (2003).
16. A. D. Koulouklidis, C. Lanara, C. Daskalaki, *et al.*, "Impact of gas dynamics on laser filamentation THz sources at high repetition rates," Opt. Lett. **45**, 6835 (2020).
17. J. Bernhardt, W. Liu, F. Théberge, *et al.*, "Spectroscopic analysis of femtosecond laser plasma filament in air," Opt. Commun. **281**, 1268 (2008).
18. L. A. Finney, P. J. Skrodzki, M. Burger, *et al.*, "Optical emission from ultrafast laser filament-produced air plasmas in the multiple filament regime," Opt. Express **26**, 29110 (2018).
19. O. Balachninaitė, J. Skruibis, A. Matijošius, *et al.*, "Temporal and spatial properties of plasma induced by infrared femtosecond laser pulses in air," Plasma Sources Sci. Technol. **31**, 045001 (2022).
20. A. Higginson, Y. Wang, H. Chi, *et al.*, "Wake dynamics of air filaments generated by high-energy picosecond laser pulses at 1 kHz repetition rate," Opt. Lett. **46**, 5449 (2021).
21. J. Xue, N. Zhang, L. Guo, *et al.*, "Effect of laser repetition rate on the fluorescence characteristic of a long-distance femtosecond laser filament," Opt. Lett. **47**, 5676 (2022).
22. F. Yin, J. Long, Y. Liu, *et al.*, "Pulse repetition-rate effect on the intensity inside a femtosecond laser filament in air," High Power Laser Sci. Eng. **11**, e46 (2023).
23. T.-J. Wang, M. H. Ebrahim, I. Afxenti, *et al.*, "Cumulative effects in 100 kHz repetition-rate laser-induced plasma filaments in air," Adv. Photon. Res. **4**, 2200338 (2023).
24. H. Zheng, F. Yin, T.-J. Wang, *et al.*, "Time-resolved measurements of electron density and plasma diameter of 1 kHz femtosecond laser filament in air," Chin. Opt. Lett. **20**, 093201 (2022).
25. H. R. Griem, *Plasma Spectroscopy* (McGraw-Hill, 1964).
26. G. Point, E. Thouin, A. Mysyrowicz, *et al.*, "Energy deposition from focused terawatt laser pulses in air undergoing multifilamentation," Opt. Express **24**, 6271 (2016).
27. Y.-H. Cheng, J. K. Wahlstrand, N. Jhajj, *et al.*, "The effect of long timescale gas dynamics on femtosecond filamentation," Opt. Express **21**, 4740 (2013).
28. J. K. Wahlstrand, N. Jhajj, and H. M. Milchberg, "Controlling femtosecond filament propagation using externally driven gas motion," Opt. Lett. **44**, 199 (2019).
29. C. Aragón and J. A. Aguilera, "Characterization of laser induced plasmas by optical emission spectroscopy: a review of experiments and methods," Spectrochim. Acta, Part B: Atomic Spectros. **63**, 893 (2008).
30. R. W. P. McWhirter, *Plasma Diagnostic Techniques*, R. H. Huddlestone and Stanley L. Leonard, eds. (Academic, 1965).
31. https://www.nist.gov/pml/atomic-spectra-database.